31st Annual International Conference of the IEEE EMBS
Minneapolis, Minnesota, USA, September 2-6, 2009

Partial directed coherence-based information flow in Parkinson's disease patients performing a visually-guided motor task

G. Tropini, J. Chiang, *Member, IEEE,* Z.J Wang, *Member, IEEE,* M.J. McKeown.

Abstract- We propose a partial directed coherence (PCD) method based on a sparse multivariate autoregressive (mAR) model to investigate patterns of information flow in electroencephalography (EEG) recordings in Parkinson's disease (PD) patients performing a visually-guided motor task. The use of a sparsity constraint on the mAR matrix addresses issues such as sample size, model order selection and number of parameters to be estimated, particularly when the number of EEG channels used is large and the window size is small in order to capture dynamic changes. The proposed PDC-based information flow analysis demonstrated distinctly altered patterns of connectivity between PD patients off medication and healthy subjects, particularly with respect to net information outflow from the left sensorimotor (L Sm) region, which might indicate excessive spreading of activity in the diseased state. Disrupted patterns of connectivity in PD were partially restored by levodopa medication. In addition, PDC-based analysis proved to be more sensitive to temporally-dynamic connectivity changes as compared to traditional spectral analysis, which might be influenced primarily by large-scale changes. We suggest that the proposed sparse-PDC method is a suitable technique to investigate altered connectivity in Parkinson's disease.

I. INTRODUCTION

Recent trends in neurobiology and signal processing research show an increased interest in understanding the functional connectivity of brain regions that can be inferred from electroencephalography (EEG) data. Since the EEG remains the most widespread technology capable of recording brain activity at msec resolution, several mathematical methods have been proposed to infer connectivity changes that occur at rapid time scales, such as correlation, coherence and Granger causality [1, 2].

Disrupted brain connectivity is being increasingly recognized in pathological conditions such as Parkinson's disease, epilepsy, schizophrenia and Alzheimer's Disorder (AD) [3-5].

Parkinson's disease (PD) is an excellent model to assess abnormal synchronization and connectivity in humans. Patients undergoing surgery for deep brain stimulation (DBS) have electrodes placed in deep brain structures such as the subthalamic nucleus (STN), providing a unique opportunity to assess local field potential (LFP) oscillatory behavior in brain circuits that are not normally accessible by non-invasive (scalp) EEG recordings. These neuronal recordings demonstrate abnormal synchronization of neuronal activity within basal ganglia (BG) structures such as the STN and the globus pallidus external (GPe) [4]. In particular, excessive synchronization in the β-band (13-30 Hz) in these brain structures appears to suppress movement and could thus be involved in PD symptoms such bradykinesia (slowness of movement) [4,6,7]. Moreover, the PD state results in large-scale oscillatory activity that can readily propagate through the BG circuitry and spread to numerous cortical areas through BG-thalamocortical connections [7-9], and therefore the EEG might be an accurate, albeit indirect, marker of abnormal BG oscillations, despite the fact that it still largely reflects cortical activity. Most significantly, work in PD patients undergoing DBS surgery of the STN and performing a choice reaction task has shown that patterns of event related synchronization (ERS) and desynchronization (ERD) in the α and β-bands were robustly detected simultaneously in both scalp and depth recordings [10].

In order to investigate functional connectivity changes in PD, we employed a partial directed coherence (PDC) based methodology. Traditional methods of EEG analysis such as coherence and Granger causality (GC) are limited by the fact that they can only investigate pair-wise connectivity while neglecting the possible influence(s) from other nodes. While coherence is unable to identify the direction of information flow between cortical regions [1], GC is capable of this distinction. GC is based on comparing the variance of residuals from a scalar autoregressive (AR) application to one signal $x(t)$, with that from a bivariate AR application to $x(t)$ and a potentially driving signal $y(t)$ [11]. However, traditionally GC has only been used in multiple pair-wise analyses when considering the multichannel case [2].

To overcome these limitations, partial directed coherence (PDC) examines multi-channel time series and allows the simultaneous modeling of all channels with a multivariate autoregressive (mAR) model [2]. Moreover, since neural signals often exhibit frequency-specific oscillatory activity, the ability to provide spectral information of causal relations makes PDC an attractive tool for neuroscience studies.

G. Tropini and M. J. McKeown are with the Pacific Parkinson's Research Centre, University of British Columbia, Vancouver, Canada. E-mail: giorgiat@interchange.ubc.ca, mmckeown@interchange.ubc.ca.

J. Chiang and Z. J. Wang are with the Department of Electrical and Computer Engineering, University of British Columbia, Vancouver, Canada. E-mail: joycehc@interchange.ubc.ca, zjanew@interchange.ubc.ca .
This work was funded by a Michael Smith Foundation for Health Research (MSFHR) Clinical Junior Graduate Studentship (G.T.), a CIHR Frederick Banting and Charles Best Canada Graduate Scholarship, Master's Award (G.T.), and a MSFHR Team Start-up Grant (M.J.M.).

Finally, since PDC takes into account influences of all other channels when assessing the connectivity between any given pair of signals, it will be more robust to volume conduction effects that may affect standard coherence techniques.

However, the computation of PDC poses several technical challenges in real applications, especially when the number of EEG channels of interest is relatively large in practice (e.g. ~20). As noted in [1], the successful estimation of PDC critically depends upon the proper fitting of the mAR model to the data, which in turn is dependent upon the number of channels, optimal mAR model order selection and sample sizes of the training data. In general, a higher model order allows more intricate data dynamics to be captured and gives a higher frequency resolution, but at the expense of a greater number of parameters to be estimated.

Furthermore, the full-connectivity assumption of PDC analysis may be questionable in EEG results, as the EEG typically demonstrates "small world" network properties, i.e. most nodes are not directly connected to one another, but long range connections between local clusters of nodes can be present [12-13]. Additionally, a sparse model requires the estimation of fewer parameters, of critical importance when data samples are at a premium.

The above observations motivated us to incorporate a sparse mAR model into the current PDC technique as has recently been suggested for fMRI analysis [14]. In this paper, we utilized a sparse mAR-based PDC technique in which PDC estimates are derived from sparse mAR coefficient matrices given by penalized regression. Penalized regression effectively reduces the number of free parameters to be estimated, which is particularly important when the data are of limited sample size.

The sparse-mAR based PDC model was used to determine patterns of information flow in PD patients performing a visually guided joystick task. This task has previously been shown to modulate β-band synchronization of local field potential (LFP) recordings of PD patients undergoing DBS surgery [15].

II. METHODS

We first review traditional multivariate autoregressive models and least square-based parameter estimation techniques.

A. Sparse mAR Model

In a regular mAR model, the multivariate time series at each time point is represented as a linear, weighted sum of its previous time points, and it can be formulated as

$$\mathbf{y}(t) = \sum_{r=1}^{P} \mathbf{A}_r \mathbf{y}(t-r) + \mathbf{e}(t) \qquad (1)$$

where the observation $\boldsymbol{y(t)}$ is a d-dimensional vector at time t, p denotes the order of the mAR model, and the vector $\boldsymbol{e(t)}$ represents white Gaussian noise. The mAR coefficient $\boldsymbol{A}_r$ is a $d \times d$ matrix, where the element $\boldsymbol{A}_r(i,j)$ measures the influence that variable j exerts on variable i after r time points. In a regression framework, Eqn 1 can be rewritten as

$$\mathbf{Z} = \mathbf{X}\beta + \mathbf{E} \qquad (2)$$

where:

$$\begin{aligned}
\mathbf{Z} &= \mathbf{Y}_{p+1:N} \\
&= [\mathbf{y}(p+1), \mathbf{y}(p+2), \ldots, \mathbf{y}(N)]^T, \\
\mathbf{X} &= [\mathbf{Y}_{p:N-1}, \mathbf{Y}_{p-1:N-2}, \ldots, \mathbf{Y}_{1:N-p}], \\
\beta &= [\mathbf{A}_1, \mathbf{A}_2, \ldots, \mathbf{A}_p]^T, \\
\mathbf{E} &= [\mathbf{e}(p+1), \mathbf{e}(p+2), \ldots \mathbf{e}(N)]^T.
\end{aligned}$$

Equation (2) can be solved using the maximum likelihood (ML) approach. Under the iid (independent and identically distributed) white noise assumption of ***E,*** this is equivalent to minimizing the mean square error:

$$\hat{\beta} = \arg\min_{\beta} \left\| (\mathbf{Z} - \mathbf{X}\beta) \right\|^2. \qquad (3)$$

It is worth emphasizing that the performance of the ML estimator is highly dependent on the sample size N and the number of parameters to be estimated. In real applications, the available data points are often limited, which in turn leads to poor estimation accuracy. Furthermore, the estimated coefficients yielded by the least square (LS) approach in (3) are typically non-zero, which makes neurobiological interpretation of results (e.g. identifying brain connectivity patterns in EEG studies) difficult. Such non-zero observations are also against the sparsity assumption in brain connectivity networks.

To address these issues, a possible solution is to impose sparsity constraint on the mAR coefficients (i.e. $\boldsymbol{A}_r$ matrix) and perform variable selection using penalized regression methods [14]. The basic idea of penalized regression is to maximize the likelihood while at the same time, penalize complex models. In mathematical terms, penalized regression can be expressed as the minimization of the penalized least square function:

$$\hat{\beta} = \arg\min_{\beta} \left\| (\mathbf{Z} - \mathbf{X}\beta) \right\|^2 + \lambda^2 \sum_{i=1}^{d} p(|\beta_j|), \qquad (4)$$

where λ is the regularization parameter. We determine the value of λ using the Bayesian information criterion (BIC). Several different penalty functions have been introduced in the literature, including ridge, LASSO and SCAD. An overview of these penalty functions can be found in [16]. Here we use the popular LASSO penalization

$$p(|\beta_j|) = |\beta_j|, \qquad (5)$$

because of its ability to automatically set small coefficients to zero, which effectively yields sparse solutions [16].

To solve the optimization problem in (4), we use a Local Quadratic Approximation (LQA) algorithm, proposed by Fan and Li [16]. LQA first casts the problem of penalized least square minimization presented in Eqn. 4 into a penalized likelihood maximization problem. It further

addresses the issue of singularity at the origin that exists in penalty functions such as LASSO and SCAD by locally approximating „$p(|\beta_j|)$" with a quadratic function. The resulting penalized likelihood function becomes both differentiable and concave, and it can be easily solved using gradient-based optimization methods such as the Newton-Raphson algorithm. A detailed description of the LQA algorithm can be found in [16].

B. Partial Directed Coherence

PDC can be considered as the frequency-domain representation of Granger causality. It involves the transformation of the mAR coefficients in (2) into the frequency domain via the Fourier transform

$$\bar{\mathbf{A}}(f) = \mathbf{I} - \sum_{r=1}^{p} \mathbf{A}_r e^{-i2\pi fr} \tag{6}$$

where $\boldsymbol{I}$ is a d x d identity matrix. The estimate of PDC from the node y_i to the node y_j is defined as

$$\pi_{y_j \leftarrow y_i}(f) = \frac{\bar{A}_{j,i}(f)}{\sqrt{\sum_{m=1}^{d} |\bar{A}_{m,i}(f)|^2}}. \tag{7}$$

PDC takes on a value between 0 and 1, and describes the pairwise relatedness between y_i and y_j as a function of frequency after discounting the effect of other simultaneously observed series.

C. Subjects

Nine volunteers with mild to moderately severe, clinically diagnosed PD participated in our study. All patients stopped their levodopa medication overnight for a minimum of 12hrs before the study. We also recruited nine healthy aged-matched volunteers without active neurological disorders. In each group, eight subjects were right-handed and one was left-handed.

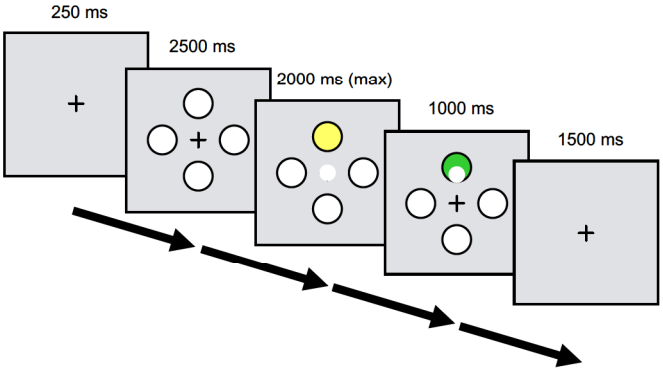

Fig. 1. Visually guided choice reaction paradigm.

D. Experimental Design and Data Collection

Subjects performed a visually guided joystick task [15]. Briefly, subjects had to use a joystick with their dominant hand to select one of four randomly activated (yellow) targets as quickly as possible (Fig. 1). Targets turned green once they were correctly selected. A total of 68 trials were presented, with an equal number of targets in each direction. Target presentation was pseudo-randomized so that the same sequence of trials was presented to each subject.

Subjects were fitted with an EEG cap with 20 active channels using the international 10-20 placement system, referenced to the mastoids. Artifacts due to eye movements were recorded by surface electrodes placed above and below the eyes. Data were recorded at 1000 Hz and aligned to task-related events via TTL pulse timestamps sent from the stimulus computer (via Matlab commands) to the EEG system through the parallel port.

E. Data Analysis

Data were down-sampled to 250Hz, and eye and EMG-derived artifacts were removed via the Automatic Artifact Removal (AAR) toolbox v1.3 (Release 09.12, Gomez-Herrero 2007) of the EEGLab open source Matlab Toolbox [17]. The denoised data were then bandpassed at 1-100 Hz. Next, data were normalized to unit variance and subsequently averaged over four electrode regions {*Fronto-central (F-Central)*: Fp1, Fp2, F3, F4, F7, F8, Fz, *Left sensorimotor (L Sm)*: C3, P3, T7, P7, *Right sensorimotor (R Sm)*: C4, P4, T8, P8, and *Central*: Cz, Pz}.

F.1. Spectral analysis

For each subject group (Normals, PD) and each subject, trials were analyzed separately by computing spectrograms over the 0-50 Hz frequency range for each individual trial.

For analysis purposes, a trial was defined as the time from the initial presentation of the fixation cross to the end of the immediately following inter-trial interval (i.e. from cross to cross as depicted in Fig. 1). The window size used was 32 samples and the window was 16.

Individual trial spectrograms for each electrode region were then averaged across all subjects within one group. In order to ensure that trials were all the same length, they were truncated to the shortest trial length (5.816 s).

F.2. Sparse mAR-based PDC analysis

Information flow between pairs of electrode regions was determined by computing the PDC spectrum, based on a 5th order sparse mAR model as described in Sections II A-B, for each individual trial. In order to ensure that trials were all the same length, they were again truncated to the shortest trial length as described above. The window size for the PDC spectrum analysis was 120 samples (= 0.48s) and the window shift 16 samples (= 0.064s) and the PDC was computed over the 0-50 Hz frequency range. Individual trial PDC spectrograms (PDCograms) were then averaged across all subjects within each group, for each direction of flow between pairs of electrode regions (e.g. L Sm→F-Central, and F-Central→L Sm).

To assess the statistical significance of the PDC changes, we integrated the PDC in the 15-30Hz band and calculated

the difference between the PDC before subjects were moving the joystick and the ~1-s they were moving the joystick for each trial. A two-way ANOVA with subject and group factors was computed. Level of significance was set at p = 0.0260, corresponding to p = 0.05 with an FDR correction.

We then sought to determine the overall information flow into and out of each electrode region. For each region of interest, the sum of the average information flow towards each of the remaining regions was subtracted from the sum of the average information flow into the region of interest over the 0-50 Hz frequency range and over the length of a trial. The final values were then displayed as Delta PDCograms, where positive values in the color map indicate net flow of information **into** the region of interest, while negative values indicate information **outflow** from the same region.

III. RESULTS

A. Spectral Analysis

The spectral analysis showed a decrease in β-band power over the 15-30 Hz range in correspondence to the onset of the "Go" cue in the F-Central, L Sm and R Sm regions (Fig. 3). This β band power decrease was especially evident in the normal subjects, and rebounded to rest levels in correspondence to the end of movement. In contrast, blunted modulation was present at the same latency in PD subjects. The ANOVA test found significant group effects in L_Sm→ F-Central and F-Central → L_Sm connections.

Spectral analysis of the Central region in control subjects showed increased power in the 0-10 Hz range in correspondence to movement. The overall power in the Central region was also decreased as compared to the power in the other regions. In PD, there was an overall increase in 0-10 Hz power across the entire trial, although a modest power increase, mimicking that seen in control subjects, was also observed in correspondence to movement.

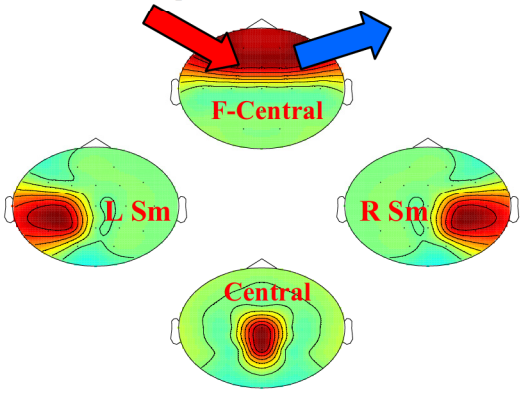

Fig. 2. Representation of the information flow into and out of the regions of interest (*F-Central, L Sm, R Sm, Central*). As depicted in the Delta PDCograms (Fig. 4), colours in the red range (positive values) represent net inflow, while colours in the blue range (negative values) represent net outflow.

B. PDC-based Information Flow Analysis

Information flow analysis revealed striking differences between control subjects and PD subjects, particularly with respect to net inflow and outflow to the L Sm and Central regions (Fig. 4).In control subjects, a net outflow in the 10-20 Hz range was observed in the L Sm region, while a net inflow was present in higher (>35 Hz) and lower (<10Hz) frequency ranges. In contrast, PD subjects showed an increased outflow in the 10-20 Hz range, and a corresponding decreased inflow in the same higher and lower frequency ranges.

Interestingly, the patterns of information flow in the Central region reverse-mirrored those observed in the L Sm region. In particular, the net inflow pattern in the 10-20 Hz range observed in the control group was greatly increased in the PD group, except during the peri-movement interval. PD subjects also showed an increased inflow to the R Sm region in the <10 Hz frequency range as compared to normal subjects. Moreover, PD subjects showed an increased net inflow to the F-Central region over a wide frequency range (> 30 Hz) as compared to control subjects.

The pair-wise flow analysis shown in the individual PDCograms (Fig. 3) also revealed peculiar patterns of information flow, particularly with respect to the L and R Sm areas and the F-Central region. In PD subjects, the bi-directional flow between the L and R Sm areas was in fact greatly decreased as compared to control subjects at frequencies <20 Hz. In addition, PDC analysis revealed asymmetry in pairwise connectivity between the L Sm and F-Central region in normal subjects. In fact, the decrease in β power observed during movement rebounded much later in the L Sm→ F-Central direction of flow as compared to the F-Central→ L Sm connection. This pattern of connectivity may underlie the greater drive from motor areas recruited by the task to the frontal and prefrontal areas not only during the movement phase but also in the recovery phase immediately following completion of the task.

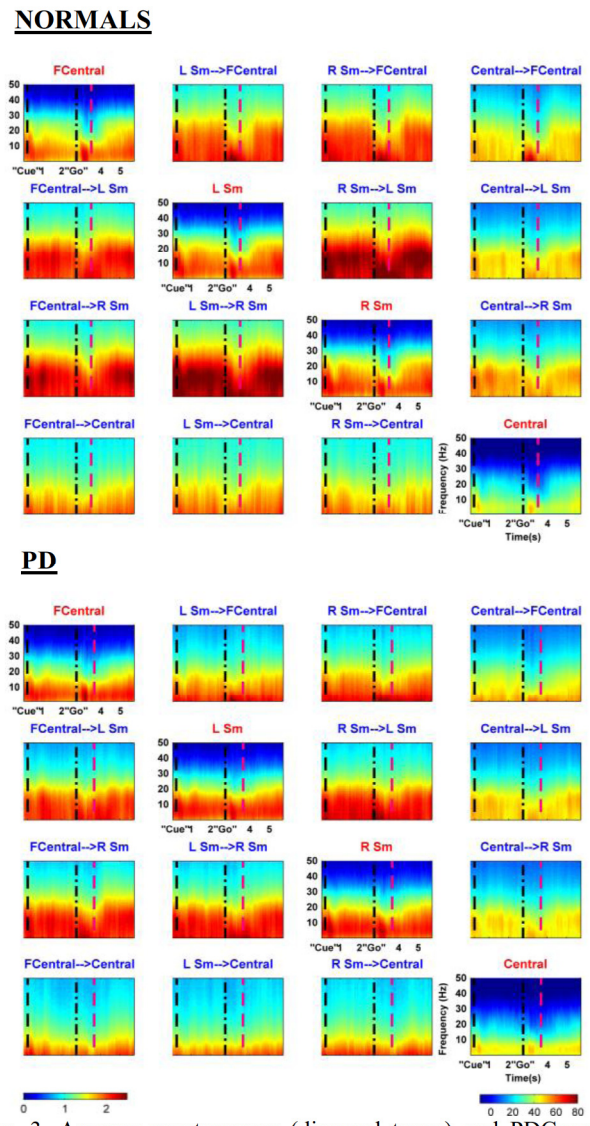

Fig. 3. Average spectrograms (diagonal terms) and PDCograms (non-diagonal terms) for each electrode region. Red vertical bars indicate the mean reaction times. "Cue" indicates presentation of the target circles, while "Go" indicates the target activation.

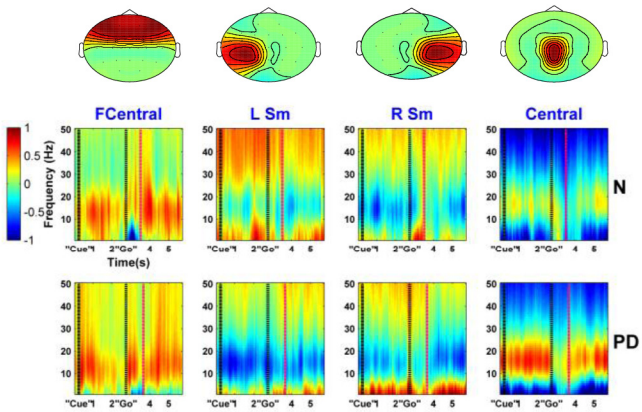

Fig. 4. Average information flow into the electrode regions of interest for all subject groups. Positive values indicate net inflow, while negative values indicate net outflow. Red vertical bars indicate the mean reaction times. "Cue" indicates presentation of the target circles, while "Go" indicates the target activation.

DISCUSSION

Our results indicate that healthy and PD subjects show considerable differences in the modulation of β band activity. While control subjects down-regulate β power during movement, PD subjects are unable to similarly modulate activity in this frequency range. This result is consistent with LFP studies that have suggested that excessive synchronization in the β band in PD subjects might have an anti-kinetic effect, thus being responsible for PD symptoms such as bradykinesia (slowness of movement) [4,6,7]. From a behavioral point of view, the PD-affected individuals showed increased reaction times (albeit not significantly) as compared to the control group (PD: 0.91 ± 0.12 s, Normals: 0.76 ± 0.16 s).

The observed increase in net outflow from the L Sm region in the diseased state might indicate an excessive spread of activation from the primary motor areas involved in the contralateral movement, to neighboring regions. For example, current fMRI work in our group has demonstrated a wider spread of activation in PD subjects (as measured by amplitude and spatial variance in the BOLD response) in bilateral cerebellar hemispheres, primary motor cortex (M1) and supplementary motor area (SMA) during a visuo-motor tracking task using a pressure-responsive bulb [18]. Previous cognitive studies have also shown a wider spread of activation in the prefrontal cortex of PD subjects off medication [19]. Thus, while it might be difficult - in part due to the nature of EEG data itself - to assess with certainty the absolute significance of neuronal activity modulation during a motor task, our results appear to be consistent with a body of knowledge that involved the use of different experimental techniques (fMRI, LFP recordings).

Overall, our results suggest that the use of a sparse mAR, PDC-based technique might be better-suited than spectral analysis to detect information flow changes between brain regions.The PDC-based information flow analysis was in fact able to reveal patterns of connectivity otherwise undetectable through simple spectral analysis, given that spectral analysis patterns were not considerably different across most regions (in particular F-Central, L Sm and R Sm) for a given subject group. Thus, spectral analysis might be primarily sensitive to large-scale power changes, and therefore might not reveal specific patterns of information flow between different brain regions, that might differ in the normal and diseased states.

In addition, the use of a sparse mAR model is invaluable in that the sparsity constraint reduces the risk of over-fitting the data, thus leading to higher sensitivity in the detection of connectivity changes that can occur during a motor task. This is especially true given that activity modulation across the motor task interval is quite rapid (even as detected by

spectral analysis), and thus short window sizes are needed to allow sufficient temporal resolution, which can lead to a significant increase in the number of parameters to be estimated.

In order to reduce computational demands, we employed an averaging method to reduce the number of nodes used in the mAR model and obtain a limited number of regions of interest but we are currently exploring other ways to better define these brain areas, such as for example the use of ICA-based techniques. To further reduce the number of parameters to be estimated, only four areas of interest were included in our study, since they were most relevant to the analysis of the motor task presented in our study. However, future averaging or clustering methods might allow us to better identify other potential regions of interest.

Overall, the use of a sparse mAR-based PDC technique was able to reveal patterns of information flow that are quite different between healthy controls and PD subjects, and that would not otherwise be revealed by traditional spectral analysis methods. Although future work is needed to further optimize the choice of electrode regions or nodes used in the analysis, sparse mAR-based PDC appears to be well-suited to detect temporally-sensitive connectivity changes in both the healthy and the diseased state. Thus, this technique might be applicable to the investigation of brain activity patterns in other neurological conditions, such as epilepsy or schizophrenia, which are characterized by rapid and/or task-dependent connectivity changes.

IV. ACKNOWLEDGMENT

The authors would like to thank Dr. Edna Ty and Vignan Yogendrakumar for assistance in patient recruitment and data collection.

V. REFERENCES

[1] E. Pereda, R. Quiroga, and J. Bhattacharya, "Nonlinear multivariate analysis of neurophysiological signals," *Progress in Neurobiology*, vol. 77, no. 1-2, pp. 1–37, 2005.

[2] L. Baccalá and K. Sameshima, "Partial directed coherence: a new concept in neural structure determination", *Biological Cybernetics*, vol. 84, no. 6, pp. 463–474, 2001.

[3] F. Varela, J.P. Lachaux, E. Rodriguez and J. Martinerie, "The brainweb: phase synchronization and large scale integration," *Nature Reviews Neuroscience*, vol. 2, no. 4, pp. 229-39, Apr. 2001.

[4] P. Brown and D. Williams, "Basal ganglia local field potential activity: character and functional significance in the human," *Clinical Neurophysiology*, vol. 116, no. 11, pp. 2510-9, Nov. 2005.

[5] A.K. Engel and W. Singer, "Temporal binding and the neural correlates of sensory awareness," *Trends in Cognitive Sciences*, vol. 5, no. 1, Jan. 2001.

[6] P. Brown, "Bad oscillations in Parkinson's disease," Jounal of Neural Transmission Supplement, no. 70, pp. 27-30, 2006.

[7] P. Gatev, O. Darbin and T. Wichmann, "Oscillations in the basal ganglia under normal conditions and in movement disorders," *Movement Disorders*, vol. 21, no. 10, pp. 1566-77, Oct. 2006.

[8] P.J. Magill, A. Sharott, J.P. Bolam and P. Brown, "Delayed synchronization of activity in cortex and subthalamic nucleus following cortical stimulation in the rat," *Journal of Physiology*, vol. 574, Pt. 3, pp. 929-46, Aug. 2006.

[9] K.Y. Tseng, F. Kasanets, L. Kargieman, L.A. Riquelme and M.G. Murer, "Cortical slow oscillatory activity is reflected in the membrane potential and spike trains of striatal neurons in rats with chronic nigrostriatal lesions," *Journal of Neuroscience*, vol. 21, no. 16, pp. 6430-9, Aug. 2001.

[10] K. Klostermann et al., "Task-related differential dynamics of EEG alpha- and β-band synchronization in cortico-basal motor structures," *European Journal of Neuroscience*, vol. 25, no. 5, pp. 1604-15, Mar. 2007.

[11] M. Ding, Y. Chen, and S. L. Bressler, "Granger causality: basic theory and application to neuroscience," Handbook of Time Series Analysis, Wiley-VCH Verlage, vol. 2006, pp. 437–460.

[12] R. Ferri, F. Rundo, O. Bruni, M.G. Terzano, C.J. Stam, "The functional connectivity connectivity of different EEG bands moves towards small-world network organization during sleep,", *Journal of Clinical Neurophysiology*, vol. 199, no. 9, pp. 2026-36, Sep. 2008.

[13] S. Micheloyannis, E. Pachou , C.J. Stam, M. Vourkas, S. Erimaki, V. Tsirka, "Using graph theoretical analysis of multi channel EEG to evaluate the neural efficiency hypothesis,", *Neuroscience Letters*, vol. 402, no. 3, pp. 273-7, Jul. 2006.

[14] P. Valdes-Sosa, J. Sanchez-Bornot, A. Lage-Castellanos, M. Vega-Hernandez, J. Bosch-Bayard, L. Melie-Garcıa, andE. Canales-Rodr´ıguez, "Estimating brain functional connectivity with sparse multivariate autoregression," Philosophical Transactions of the Royal Society B: Biological Sciences, vol. 360, no.1457, pp. 969–981, 2005.

[15] R. Amirnovin, Z.M. Williams, G.R. Cosgrove, E.N. Eskandar, "Visually guided movements suppress subthalamic oscillations in Parkinson's disease patients," *Journal of Neuroscience,* vol. 24, no. 50, pp. 11302-6, Dec. 2004.

[16] J. Fan and R. Li, "Variable Selection via Non concave Penalized Likelihood and its Oracle Properties," Journal of the American Statistical Association, vol. 96, no. 456, pp. 1348–1360, 2001.

[17] A. Delorme and S. Makeig, "EEGLAB: an open source toolbox for analysis of single-trial EEG dynamics," Journal of Neuroscience Methods, vol 134, pp. 9-21, 2004.

[18] B. Ng, S.J. Palmer, R. Aburghabieh, M.J.McKeown, "Focusing effects of L-dopa in Parkinson's disease,", Human Brain Mapping (in press).

[19] O. Monchi, M. Petrides, J. Doyon, R.B. Postuma, K. Worsley, A. Dagher, . "Neural bases of set-shifting deficits in Parkinson's disease," Journal of Neuroscience, vol. 24, no. 3, pp. 702-10, Jan 2004.